Dynamics of the N-Terminal α-Helix Unfolding in the Photoreversion Reaction of Phytochrome *A*†

Eefei Chen,‡ Veniamin N. Lapko,§ Pill-Soon Song,§ and David S. Kliger*,‡

Department of Chemistry and Biochemistry, University of California, Santa Cruz, California 95064, and Department of Chemistry, University of Nebraska, Lincoln, Nebraska 68588

Received October 29, 1996; Revised Manuscript Received February 19, 1997⊗

ABSTRACT: Time-resolved circular dichroism spectroscopy in the far-UV spectral region was used to examine the intermediates of the phytochrome photoreversion reaction (Pfr → Pr). Three intermediates, lumi-F (τ = 320 ns), meta-Fa (τ = 265 μs) and meta-Fb (τ = 5.5 ms), have been identified in a simple sequential kinetic photoreversion mechanism by absorption spectroscopy [Linschitz, H., Kasche, V., Butler, W. L., & Siegelman, H. W. (1966) *J. Biol. Chem. 241*, 3395−3403; Pratt, L. H., & Butler, W. L. (1968) *Photochem. Photobiol. 8*, 477−485; Burke, M., Pratt, D. C., & Moscowitz, A. (1972) *Biochemistry 11*, 4025−4031; Spruit, C. J. P., Kendrick, R. E., & Cooke, R. J. (1975) *Planta (Berlin) 127*, 121−132; Eilfeld, P., & Rüdiger, W. (1985) *Z. Naturforsch. 40c*, 109−114; Chen, E., Lapko, V. N., Lewis, J. W., Song, P.-S., & Kliger, D. S. (1996) *Biochemistry 35*, 843−850]. In order to correlate the unfolding of the N-terminal α-helical segment with one or more of the intermediate species, time-resolved methods were coupled with the structurally sensitive probe of CD in the far-UV spectral region. Analysis of the TRCD data associates the decrease in α-helical content that occurs upon formation of Pr with decay of the meta-Fa intermediate. This unfolding process occurs with a time constant of 310 ± 125 μs, which is consistent with the 265-μs lifetime for meta-Fa.

Photosensory pigments help maintain a plant's physiological well-being by sensing changes in environmental light conditions and signaling for an appropriate response. One of the best-characterized photoreceptors is phytochrome *A* (phy*A*), which is known to play a regulatory role in the developmental process of photomorphogenesis (including gene expression, chlorophyll synthesis, flowering, and germination). Phy*A*'s role as a light switch is based on a reversible phototrigger mechanism that is sensitive to variations in far-red and red light in the environment. When light of 660 nm is absorbed, phy*A* is activated to a switch-on form (Pfr), whereas light of 730 nm causes Pfr to revert to a switch-off form (Pr). The underlying structural and molecular basis of physiological activity, which is maintained by the balance of Pr and Pfr, has been the focus of many studies [for a recent review see Sineshchekov (1995)]. Thus, there is a considerable understanding of the equilibrium Pr and Pfr structures, and several intermediates that are involved in the activation and inactivation mechanisms have been detected.

Oat phy*A* is a 124 kDa protein containing an open tetrapyrrole chromophore covalently linked through a thioether bond to Cys-321 (Lagarias & Rapoport, 1980). Two major domains have been identified in the phy*A* protein, a ∼70 kDa N-terminal domain that binds the chromophore and a ∼55 kDa C-terminal domain that is required for dimerization (Lagarias & Mercurio, 1985; Jones & Quail, 1986). Both polypeptide regions contain segments that are necessary for photobiological function. Additionally, many studies have focused on a 6 kDa segment within the N-terminal domain that undergoes light-induced conformational changes and is essential for physiological activity (Cherry et al., 1992; Stockhaus et al., 1992). The N-terminal end is comprised of two hydrophilic regions, rich in serine and threonine residues, that are separated by a short hydrophobic segment. Folding and unfolding of the 6 kDa α-helix encompasses the short hydrophobic and the second hydrophilic segments, which apparently involve amino acid residues 20−50 (Parker et al., 1991). Interaction of the N-terminus with the chromophore is likely to be stabilized by the presence of the 6 kDa subdomain α-helix (Vierstra & Quail, 1982; Vierstra et al., 1987; Jones et al., 1985; Cordonnier et al., 1985; Cherry et al., 1991, 1992). *Z,Z,Z* to *Z,Z,E* isomerization of the 15,16-double bond in the chromophore (Rüdiger et al., 1983; Farrens et al., 1989; Fodor et al., 1990; Siebert et al., 1990; Hildebrandt et al., 1992) is one of the two major structural changes that occurs upon photoconversion of Pr to Pfr, the other being the formation of the N-terminal α-helix segment (Chai et al., 1987; Vierstra et al., 1987).

The dynamics of N-terminus α-helical folding have already been examined with time-resolved optical absorption (TROD) and time-resolved circular dichroism (TRCD) studies of the Pr → Pfr photoactivation reaction (Zhang et al., 1992; Björling et al., 1992). Formation of the α-helical structure has been associated with decay of the meta-Ra2 (τ = 42 ms) and/or the meta-Rc (τ > 266 ms) intermediates identified in the later stages of the Pr → Pfr reaction (Chen et al., 1993). Although five transient species were observed in the photoactivation reaction by Björling et al. (1992), the meta-Ra1 intermediate was not detected by Braslavsky et al. (private communication to P.S.S.). In the Pfr → Pr photoreversion reaction only three intermediates have been identified with low-temperature absorption and CD spectroscopies and in

† This work was supported by NIH Grants GM-35158 (D.S.K.) and GM-36956 (P.S.S.).

* To whom correspondence should be addressed.

‡ University of California.

§ University of Nebraska.

⊗ Abstract published in *Advance ACS Abstracts,* April 1, 1997.

S0006-2960(96)02706-7 CCC: $14.00

flash photoreversion studies (Linschitz et al., 1966; Pratt & Butler, 1968; Burke et al., 1972; Spruit et al., 1975; Eilfeld & Rüdiger, 1985). The time dependence of these intermediates was recently determined using TROD methods in the far-red region: lumi-F (320 ns), meta-Fa (265 μs), and meta-Fb (5.5 ms) (Chen et al., 1996). In this study far-UV TRCD methods were used to monitor the changes in the N-terminal α-helix structure that occurs upon photoreversion of Pfr to Pr. The results suggest that unfolding of the N-terminal α-helical segment follows the decay kinetics of a single intermediate. The experimental lifetime of 310 ± 125 μs strongly indicates that this intermediate corresponds to the meta-Fa species.

MATERIALS AND METHODS

Phytochrome Purification. Native 124 kDa oat phy*A* was isolated according to a modification of the method described by Chai et al. (1987). This procedure has been described briefly in Chen et al. (1996) and in detail by Lapko and Song (1995).

Experimental Protocol. In order to generate 4−6 mJ pulses (7 ns, full-width half-maximum) of 730 nm light for the photoconversion of Pfr, a Quanta Ray PDL-1 dye laser was pumped with a Quanta Ray DCR-11 Nd:YAG laser (Spectra-Physics, Mountain View, CA). The probe beam source used to monitor the spectral changes induced by photoexcitation was a xenon flash lamp. The excitation beam entered the sample cell at an angle of 15° relative to the probe beam. The TRCD apparatus has been described in detail (Zhang et al., 1993) and is discussed briefly below.

The probe beam, initially unpolarized, was collimated with a fused silica lens before passing through an MgF_2 polarizer that separates the horizontal and vertical components of linearly polarized light. The vertical component of the light is directed through a strained fused silica plate with 2−3° of retardation along an axis set at ±45° relative to the polarization axis of the incident light. This converts the probe light into left and right elliptically polarized light, respectively. With a circularly dichroic sample, the difference in absorption of left and right circularly polarized light can be determined by measuring the change in intensity polarized along the minor ellipse axis. This is done by passing the probe beam through a second MgF_2 polarizer oriented perpendicular to the original linear polarization axis. The horizontal component (minor axis) of light is collected and focused onto a 500 μm slit of a Monospec 27 spectrograph (Thermo Jarrell Ash, Franklin, MA). The spectrograph is equipped with a 300 groove mm^{-1} grating (200 nm blaze) that provides a wavelength range of ∼140 nm. The probe light is detected with a gated optical multichannel analyzer detector (OMA, model 1420 UV, EG&G PARC, Princeton, NJ), which is coupled to a pulse amplifier (model 1304, EG&G PARC) and controlled with a detector interface (model 1461, EG&G PARC). A four channel digital delay generator (DG535, Stanford Research Systems, Sunnyvale, CA) was used to synchronize the timing between the laser, probe light and detector gate.

Phy*A* samples were prepared for experiments in the far-UV region by dilution into 20 mM Tris-HCl buffer (pH 7.8) containing 0.5 mM EDTA for a final volume of 5−7 mL. The dilution factor varied so that the final concentration of the solution had absorbance values of 0.5−0.8 at 222 nm and 1−1.5 at 210 nm in a 2 mm pathlength cell. Before each experiment the sample was photoconverted between Pfr and Pr by irradiation with a high-intensity CW light (Fiber-Lite Series 180, Dolan-Jenner Industries, Inc., Lawrence, MA) that was equipped with an interference filter to select either 660 or 730 nm light. For these photoconversions, absorption spectra of Pr and Pfr were measured in order to check the purity of the samples. SAR values and A_{730}/A_{667} ratios (for Pfr) were calculated from the absorption spectra before and after dilution. Samples used in the experiments showed an SAR value of 0.9 or higher and an A_{730}/A_{667} ratio greater than 1.40. All steady state absorption spectra were measured on a Shimadzu UV-2101PC spectrophotometer using a 2 mm pathlength quartz cuvette. Steady state CD spectra in the 200−300 nm region were also obtained for Pfr and Pr in order to check that the N-terminus α-helix region exhibited the change that is expected upon photoconversion of Pfr to Pr. These steady state CD spectra were measured on the TRCD apparatus. Pr was obtained either by CW illumination of Pfr with 730 nm light or by illumination with 730 nm light from the Nd:YAG laser set at a repetition rate of 10 Hz. Pr was converted back to Pfr by using a 660 nm filter with the high-intensity CW light. Only samples that showed the appropriate steady state CD spectra for Pfr and Pr were used for TRCD experiments.

The cell used in the TRCD experiments had fused silica windows and a heating/cooling jacket for temperature control. A peristaltic pump controlled the recycled flow of sample between the cell and an iced reservoir. The sample was stabilized at ∼10 °C during the experiment. TRCD data were collected with a 10 s delay between each laser flash, during which time the sample was flowed out of the laser beam path and was simultaneously irradiated with 660 nm light from a high-intensity CW illuminator. These steps were performed to regenerate Pfr from Pr and to ensure that each laser flash resulted in photoreversion of pure Pfr. Photoreversion experiments involved TRCD measurements of Pfr and photoexcited Pfr species probed at 1.5 μs, 100 μs, 200 μs, 1 ms, 5 ms, and 1 s after irradiation of Pfr. The stability of the Pfr sample limited the number of averages that were obtained at each time delay. With the exception of data collected 1 ms after photoexcitation, where only 80 averages were recorded, 144−256 averages were collected for all other time points.

Data Analysis. The TRCD data were analyzed in the form of difference TRCD spectra, obtained by subtracting the steady state Pfr CD spectrum from the spectrum of the photoexcited Pfr species measured at each time point. A CD spectrum of the buffer solution was subtracted from both the ground state and time-resolved spectra, and the data were offset to 0 from 290−300 nm because this region does not have any detectable CD signals. The time dependence of the CD changes was analyzed using singular value decomposition (SVD) and global analysis methods. In order to have a method of determining the uncertainty of the TRCD measurements, 12 scans of 16 averages were collected at each time point for a complete set of data. A second set of data including all time points was also collected, but with only 5−8 scans of 16 averages depending on the quantity of sample remaining. In addition, SVD and global exponential fitting analyses were performed on data in the region of 218−226 and 220−225 nm. Therefore, it was possible to calculate a standard deviation of the results by analyzing

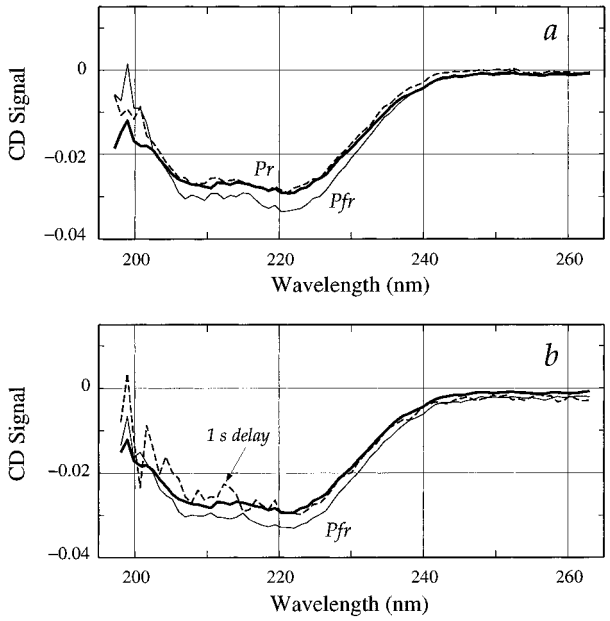

FIGURE 1: Comparison of CD spectra for Pfr and Pr. All phy*A* samples were tested for reversibility between Pfr and Pr using CW light and 10 Hz laser light sources. (a) Steady state spectrum of Pr obtained by photoconversion of Pfr with 730 nm CW light (▬) can be overlaid with the Pr spectrum that is obtained after irradiating the same sample with 730 nm light from a 10 Hz Nd:YAG laser source (- - -). The sample is reconverted to Pfr (—) by using 660 nm CW light before laser illumination. (b) TRCD spectrum obtained 1 s after the initial photoisomerization step (- - -) is similar to the spectrum measured under CW photoconversion of Pfr (—) to Pr (▬). This comparison verifies that formation of Pfr is complete by 1 s.

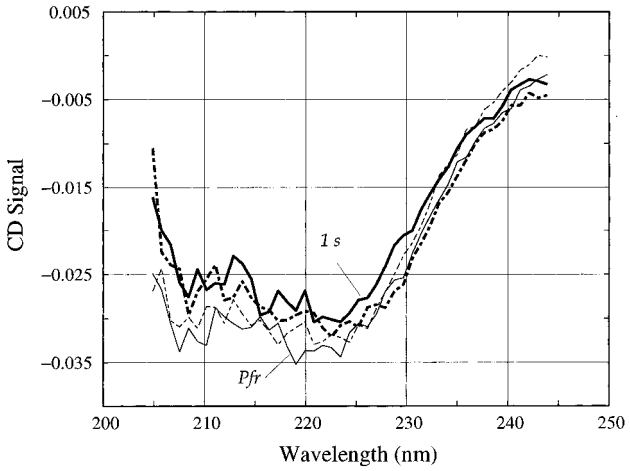

FIGURE 2: TRCD spectra of Pfr and Pfr(t). TRCD spectra were measured at 1.5, 100, and 200 μs, 1 and 5 ms, and 1 s after photoexcitation of Pfr (—). The spectra shown above were obtained at 200 μs (- - -), 5ms (▬ ▬) and 1 s (▬) delay times and represent a typical set of data. The temporal behavior of the α-helical unfolding process was fit to a single exponential, $\tau = 310 \pm 125$ μs. This time constant was calculated from the results of SVD and global kinetic analysis of all data sets.

more than one data set and by using different data analysis strategies. SVD and global analysis routines were written in the mathematical software package Matlab (Pro-Matlab, The Math Works, Inc.).

The SVD method is a matrix approach to separating experimental noise from the information about intermediate species that can be obtained from the spectral variations in the data. SVD analysis decomposes the data matrix (**A**) into mathematically independent temporal (**V**) and spectral (**U**) components. Each of these components is weighted with a singular value (**S**) that describes its importance to the data, $\mathbf{A} = \mathbf{USV}^T$. Global kinetic analysis is used to follow the temporal behavior of the spectral intermediates in the data, which are fit to a product of time (**T**) and spectral (**B**) functions, $\mathbf{A} = \mathbf{BT}$. Further details of these analysis methods have been described in related phy*A* papers (Zhang et al., 1992; Chen et al., 1996). Since the CD changes are small the data were also fit to an exponential function and compared to the results from global analysis. SigmaPlot (Version 2.01, Jandel Scientific Software, San Rafael, CA) was used to fit the data with an exponential function.

RESULTS

Figure 1 compares the CD spectra of Pfr with spectra of Pr that were measured on the TRCD apparatus after illumination of Pfr with 730 nm light from a CW source and from a 10 Hz Nd:YAG laser. All steady state CD spectra in Figure 1a were measured on the same sample to verify that the N-terminus α-helix region of the protein was responding appropriately to 730 and 660 nm light. The Pr spectra obtained from both the CW and laser methods of illumination can be overlaid, and, as expected, the magnitude of the Pr signal is ∼10% smaller than the signal for Pfr. In Figure 1b, the TRCD spectrum of Pfr, measured 1 s after photoexcitation, can be overlaid with the Pr spectra obtained using equilibrium photoconversion methods. This comparison verifies that photoconversion of Pfr to Pr is essentially complete 1 s after irradiation with 730 nm light.

Because the changes in the TRCD signals are small, only the spectra measured at 200 μs, 5 ms, and 1 s after photoexcitation are shown in Figure 2 along with the spectrum of Pfr. The difference data were analyzed in the region of 218−226 and 220−225 nm. Using SVD and global analysis methods, the time dependent CD changes were fit to a single exponential process with a lifetime of 310 ± 125 μs. It was not possible to fit a second exponential process without generating either two components of the same lifetimes or irreproducible results. The single exponential result is supported by examining the **S** matrix diagonal elements calculated using SVD and the residual spectrum at each time delay generated by global kinetic analysis. In Figure 3a, a semilog plot of the weighted value associated with each time delay distinguishes the mathematically independent components that are important to the data from the experimental noise. This plot identifies at most two spectrally significant intermediates in the process of N-terminus α-helix unfolding. The straight line in the figure indicates the behavior of the elements expected from random noise. In Figure 3b, the residuals for a single exponential fit of a representative data set are shown for each time delay in the wavelength region from about 205−225 nm. The residuals show no distinctive features that would suggest the presence of a second process. The slight rise in each spectrum in the 205 nm region for each of the time delays is attributed to a decrease in signal to noise. This problem arises from low light intensities due to the increase in absorbance by the buffer and phy*A* at wavelengths below 210 nm.

The result of the global kinetic analysis ($\tau = 310$ μs) was compared to a single exponential function, ΔCD =

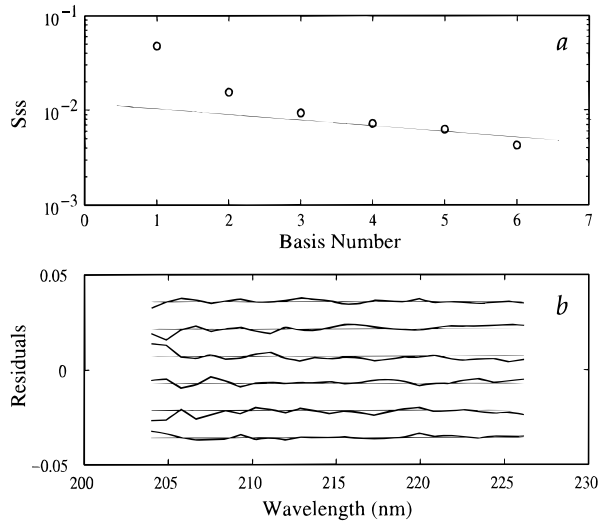

FIGURE 3: Results of SVD and global analysis of TRCD difference data. A single exponential fit of the TRCD data is supported by examination of the **S** matrix diagonal elements calculated by SVD and the residual spectrum for each time delay of the single exponential fit generated by global analysis. (a) Semilog plot of the **S** matrix elements indicates that at most two spectral intermediates can be expected to contribute significantly to the TRCD data. (b) Residual spectra for each time delay, 1.5, 100, and 200 μs, 1 and 5 ms, and 1 s after photoexcitation (top to bottom), calculated after a single exponential fit to the data. The residuals show no distinctive features that would suggest the presence of a second exponential process.

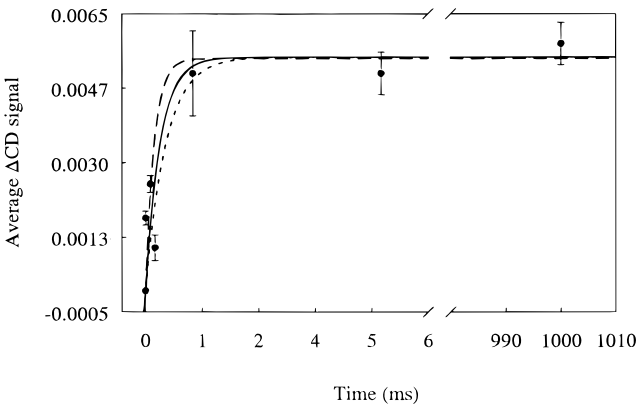

FIGURE 4: Comparison of the TRCD data to a single exponential function. The result of global kinetic analysis ($\tau = 310 \pm 125$ μs, —) is compared to a single exponential function calculated according to the equation $\Delta CD = -0.0055(e^{-t/\tau} - 1)$. A plot of the average ΔCD signal versus time shows how the changes in CD signal at 222 nm (●), along with the calculated standard deviation for each time delay, compare with the exponential fit. The exponential functions represent decay rates of 310 (—), 435 (- - -), and 185 μs (— — —).

$-0.0055(e^{-t/\tau} - 1)$, that was generated by a fit to the data. Figure 4 compares the changes in ellipticity at 222 nm to a single exponential decay with a lifetime of 310 μs. Each data point represents an average of the CD signal across the 218−226 nm wavelength range. The data are also compared to single exponential decay functions with lifetimes that correspond to the upper ($\tau = 435$ μs) and lower ($\tau = 185$ μs) limits of the standard deviation calculated for the lifetime of the change in α-helical content.

DISCUSSION

From the results of various steady state experiments on Pr and Pfr, several conformational changes are expected upon photoinitiation of the Pfr → Pr reaction. These are (1) the *Z,Z,E* to *Z,Z,Z* isomerization of the chromophore which is followed by (2) unfolding of the N-terminal helical segment, (3) an increase in the N-terminus to chromophore distance by ca. 12 Å (Farrens et al., 1992), and (4) burying of the chromophore inside the protein. These structural changes are suggested to lead to the conservation of the semi-extended chromophore configuration (Song et al., 1979; Parker et al., 1994). To correlate structural changes with the three intermediate species, lumi-F ($\tau = 320$ ns), meta-Fa ($\tau = 265$ μs), and meta-Fb ($\tau = 5.5$ ms), which are involved in a simple sequential photoreversion mechanism, time-resolved studies were coupled with the more structurally sensitive probe of CD. In these far-UV TRCD studies the dynamics of the secondary structure were monitored to identify the intermediate species that are associated with the process of N-terminal helical unfolding.

The far-UV TRCD data were fit to a single exponential process with a lifetime of 310 μs, indicating that the decrease in α-helical content is due to decay of the meta-Fa species. On the basis of the magnitude of the CD signal measured at 220 nm, formation of Pr is accompanied by a ∼10% decrease in helical structure. This change in signal is slightly larger than the previously reported 3−5% difference between Pr and Pfr observed in equilibrium CD spectra (Chai et al., 1987; Vierstra et al., 1987; Sommer et al., 1990). However, a 10% change of CD signal was also observed in the far-UV TRCD studies of the photoactivation reaction (Chen et al., 1993). These TRCD results are thought to be consistent with the equilibrium CD changes because, as previously noted (Chen et al., 1993), the magnitude of the CD change between Pr and Pfr can vary depending on the buffer system used in the experiment. In addition, it is possible that the larger change (10%) in CD signal may be due to the different purification methods used to prepare phy*A*.

Because the photoreversion reaction proceeds along a simpler and faster pathway than the photoactivation reaction, it is not necessarily surprising that unfolding of the N-terminal α-helical peptide has a faster time constant. Why the dynamics of the forward and reverse reactions differ so much can only be addressed at this stage by a comparison of the major differences in the chromophore and N-terminus of the Pr and Pfr structures. Fourier transform resonance Raman (FT-RR) spectroscopy has been used to study the structure and orientation of the Pr and Pfr chromophores. Comparison of the respective FT-RR spectra suggests that the major difference between the Pr and Pfr chromophores is not only the *Z*/*E* isomerization, but also the torsions around the two single bonds between the rings of the tetrapyrrole chromophore (Hildebrandt et al., 1992; Matysik et al., 1995). The Pr chromophore assumes a *Z,Z,Z* configuration with a twisted C9−C10 bond in the bridge between rings B and C, whereas a *Z,Z,E* geometry is found in Pfr. Although the torsion of the C9−C10 bond found in Pr is completely relaxed in Pfr, a dramatic twist around the C14−C15 bond of rings C and D introduces strain to the *Z,Z,E* configuration that is observed as a non-coplanarity of the D ring relative to the other rings of the tetrapyrrole.

The chromophore interacts with the protein through a hydrophobic chromophore "pocket" which is composed of a peptide segment, containing the chromophore binding site, surrounded by two strongly hydrophobic stretches (Eilfeld & Rüdiger, 1984; Hahn et al., 1984). The role of the

chromophore in facilitating α-helical conformations in peptide chains has been noted previously in such heme proteins as myoglobin (Beychok, 1966). In phy*A* the distance between the N-terminus and the chromophore decreases by 12 Å upon formation of Pfr. Presumably this is influenced by folding of the α-helix onto the hydrophobic chromophore pocket, which is consistent with the propensity of the 6 kDa N-terminus to form an amphiphilic helix that was demonstrated through calculations of hydrophobic moments and SDS−micelle binding tests (Parker & Song, 1990, 1992; Parker et al., 1992). Thus, the unrelaxed chromophore geometry in Pfr, as well as the conformational constraints that arise from structural ordering of the N-terminal domain and of the protein with respect to the chromophore, may be the basis for the differences observed in the Pr → Pfr and Pfr → Pr photoinduced kinetics. Without further structural characterization of the chromophore in the lumi-F and meta-Fb intermediates it is difficult to understand how the chromophore-protein interactions differ in the forward and reverse reactions to facilitate the different time constants for folding and unfolding of the α-helical peptide.

The longer time constant for folding ($\tau \geq 42$ ms) versus unfolding ($\tau = 320$ μs) of the N-terminal α-helical peptide is consistent with the idea that folding may proceed on a longer time scale because of the conformational heterogeneity of an unfolded protein (Creighton, 1993). Still, the time constant for folding is rather long for an α-helical segment that is only 6 kDa. This is probably because formation of the α-helical segment must first wait for rearrangements of the chromophore and protein to provide a favorable environment that stabilizes the function-specific N-terminal α-helix. For example, in Pfr formation of the amphiphilic α-helix is accompanied by exposure of the chromophore and the corresponding hydrophobic peptide segment of the chromophore pocket to the surrounding polar medium (Song et al., 1979; Tokutomi et al., 1981; Yamamoto & Smith, 1981; Sarkar & Song, 1982; Hahn et al., 1984; Hahn & Song, 1981; Mizutani et al., 1993). However, in Pr the unfolded N-terminal segment becomes more susceptible to the surrounding medium (Cordonnier et al., 1985; Wong et al., 1986; Jones et al., 1985), where interaction with water may prove to be more entropically favorable, while the chromophore and the hydrophobic segment of its binding site is buried in the protein.

In conclusion, analysis of the far-UV TRCD data indicates that the decrease in α-helical content that accompanies formation of Pr follows the decay kinetics of a single intermediate. The experimental lifetime of 310 μs suggests that this decay corresponds to the meta-Fa species. As observed in heme proteins such as myoglobin, the presence of the chromophore has a propensity for facilitating α-helix formation in peptide chains. Therefore, further structural characterization of the lumi-F and meta-Fb species, using TRCD methods in the far-red region, may provide insight into the influence of the chromophore on the unfolding of the α-helical segment. Comparison of these data with the chromophore interactions that facilitate α-helix folding in the forward reaction can help us understand why the time constant for unfolding is 140 times faster than for folding. The far-UV TRCD studies of the 6 kDa α-helical peptide in phy*A* provides the first kinetic measurement of both the unfolding and folding processes in a protein under near-physiological conditions. The 310-μs process is the fastest time constant that has been observed to date for peptide unfolding within a protein.

ACKNOWLEDGMENT

We thank James W. Lewis for advice and help in reviewing the manuscript.

REFERENCES

Beychok, S., (1966) *Science 154*, 1288−1299.
Björling, S. C., Zhang, C.-F., Farrens, D. L., Song, P.-S., & Kliger, D. S. (1992) *J. Am. Chem. Soc. 114*, 4581−4588.
Burke, M., Pratt, D. C., & Moscowitz, A. (1972) *Biochemistry 11*, 4025−4031.
Chai, Y.-G., Song, P.-S., Cordonnier, M.-M., & Pratt, L. H. (1987) *Biochemistry 26*, 4947−4952.
Chen, E., Parker, W., Lewis, J. W., Song, P.-S., & Kliger, D. S. (1993) *J. Am. Chem. Soc. 115*, 9854−9855.
Chen, E., Lapko, V. N., Lewis, J. W., Song, P.-S., & Kliger, D. S. (1996) *Biochemistry 35*, 843−850.
Cherry, J. R., Hondred, D., Keller, J. M., & Vierstra, R. D. (1991) in *Phytochrome Properties and Biological Actions* (Thomas, B., & Johnson, C., Eds.) NATO ASI Series H50, pp 113−126, Springer-Verlag, Berlin.
Cherry, J. R., Hondred, D., Walker, J. M., & Vierstra, R. D. (1992) *Proc. Natl. Acad. Sci. U.S.A. 89*, 5039−5043.
Cordonnier, M.-M., Greppin, H., & Pratt, L. H. (1985) *Biochemistry 24*, 3246−3253
Creighton, T. E. (1993) *Proteins: Structure and Molecular Properties*, 2nd ed., pp 309−323, W. H. Freeman and Company, New York.
Eilfeld, P., & Rüdiger, W. (1985) *Z. Naturforsch. 40c*, 109−114.
Farrens, D. L., Holt, R. E. Rospendowski, B. N., Song, P.-S., & Cotton, T. M. (1989) *J. Am. Chem. Soc. 111*, 9162−9169.
Farrens, D. L., Cordonnier, M.-M., Pratt, L. H., & Song, P.-S. (1992) *Photochem. Photobiol. 56*, 725−733.
Fodor, S. P. A., Lagarias, J. C., & Mathies, R. A. (1990) *Biochemistry 29*, 11141−11146.
Hahn, T. R., & Song, P.-S. (1981) *Biochemistry 20*, 2602−2609.
Hahn, T. R., Song, P.-S., Quail, P. H., & Vierstra, R. D. (1984) *Plant Physiol. 74*, 755−758.
Hildebrandt, P., Hoffman, A., Lindemann, P., Heibel, G., Braslavsky, S. E., Schaffner, K., & Schrader, B. (1992) *Biochemistry 31*, 7957−7962.
Jones, A. M., & Quail, P. H. (1986) *Biochemistry 25*, 2987−2995.
Jones, A. M., Vierstra, R. D., Daniels, S. M., & Quail, P. H. (1985) *Planta 164*, 501−506.
Lagarias, J. C., & Rapoport, H. (1980) *J. Am. Chem. Soc. 102*, 4821−4828.
Lagarias, J. C., & Mercurio, F. M. (1985) *J. Biol. Chem. 260*, 2415−2423.
Lapko, V. N., & Song, P.-S. (1995) *Photochem. Photobiol. 62*, 194−198.
Linschitz, H., Kasche, V., Butler, W. L., & Siegelman, H. W. (1966) *J. Biol. Chem. 241*, 3395−3403.
Matysik, J., Hildebrandt, P., Schlamann, W., Braslavsky, S. E., & Schaffner, K. (1995) *Biochemistry 34*, 10497−10507.
Mizutani, Y., Tokutomi, S., Kaminaka, S., & Kitagawa, T. (1993) *Biochemistry 32*, 6916−6922.
Parker, W., & Song, P.-S. (1990) *J. Biol. Chem. 265*, 17568−17575.
Parker, W., & Song, P.-S. (1992) *Biophys. J. 61*, 1435−1439.
Parker, W., Romanowski, M., & Song, P.-S. (1991) in *Phytochrome Properties and Biological Action*, (Thomas, B., & Johnson, C. B., Eds.) pp 85−112, Springer, Berlin.
Parker, W., Partis, M., & Song, P.-S. (1992) *Biochemistry 31*, 9413−9420.
Parker, W., Goebel, P., Ross, C. R., II, Song, P.-S., & Stezowski, J. J. (1994) *Bioconjugate Chem. 5*, 21−30.
Pratt, L. H., & Butler, W. L. (1968) *Photochem. Photobiol. 8*, 477−485.
Rüdiger, W., Thümmler, F., Cmiel, E., & Schneider, S. (1983) *Proc. Natl. Acad. U.S.A. 80*, 6244−6248.
Sarkar, H. K., & Song, P.-S. (1982) *Biochemistry 21*, 1967−1972.

Siebert, F., Grimm, R., Rüdiger, W., Schmidt, G., & Scheer, H. (1990) *Eur. J. Biochem. 194*, 921−928.
Sineshchekov, V. A. (1995) *Biochim. Biophys. Acta 1228*, 125−164.
Sommer, D., & Song, P.-S. (1990) *Biochemistry 29*, 1943−1948.
Song, P.-S., Chae, Q., & Gardner, J. D. (1979) *Biochim. Biophys. Acta. 576*, 479−495.
Spruit, C. J. P., Kendrick, R. E., & Cooke, R. J. (1975) *Planta (Berlin) 127*, 121−132.
Stockhaus, J., Nagatani, A., Halfter, U., Kay, S., Furuya, M., & Chua, N.-H. (1992) *Genes Dev. 6*, 2364−2372.
Tokutomi, S., Yamamoto, K. T., & Furuya, M. (1981) *FEBS Lett. 134*, 159−162.
Vierstra, R. D., & Quail, P. H. (1982) *Proc. Natl. Acad. Sci. U.S.A. 79*, 5272−5276.
Vierstra, R. D., Quail, P. H., Hahn, T.-R., & Song, P.-S. (1987) *Photochem. Photobiol. 45*, 429−432.
Wong, Y.-S., Cheng, H.-C., Walsh, D. A., & Lagarias, J. C. (1986) *J. Biol. Chem. 261*, 12089−12097.
Yamamoto, K. T., & Smith, W. O., Jr. (1981) *Biochim. Biophys. Acta 668*, 27−34.
Zhang, C.-F., Farrens, D. L., Björling, S. C., Song, P.-S., & Kliger, D. S. (1992) *J. Am. Chem. Soc. 114*, 4569−4580.
Zhang, C.-F., Lewis, J. W., Cerpa, R., Kuntz, I. D., & Kliger, D. S. (1993) *J. Phys. Chem. 97*, 5499−5505.

BI9627065